NPS ARCHIVE
1963
EVANS, R.

MEASUREMENTS OF THE SCATTERING MATRIX OF OBSTACLES IN MULTIMODE WAVE GUIDES

RICHARD P. EVANS

LIBRARY
U.S. NAVAL POSTGRADUATE SCHOOL
MONTEREY, CALIFORNIA

MEASUREMENT OF THE SCATTERING MATRIX OF OBSTACLES IN MULTIMODE WAVE GUIDES

* * * * * * * * * * *

Richard P. Evans

MEASUREMENT OF THE SCATTERING MATRIX OF OBSTACLES IN MULTIMODE WAVE GUIDES

by

Richard P. Evans
Lieutenant, United States Navy

Submitted in partial fulfilment of
the requirements for the degree of

MASTER OF SCIENCE
in
Aero-Electronics Engineering

United States Naval Postgraduate School
Monterey, California
June 1963

LIBRARY
U.S. NAVAL POSTGRADUATE SCHOOL
MONTEREY, CALIFORNIA

MEASUREMENT OF THE SCATTERING MATRIX OF OBSTACLES IN MULTIMODE WAVE GUIDES

by

Richard P. Evans

This work is accepted as fulfilling the thesis requirements for the degree of

MASTER OF SCIENCE
in
Aero Electronics Engineering

from the

United States Naval Postgraduate School

ABSTRACT

Accurate experimental determination of the impedance of obstacles in multimode waveguides is of continuing interest. The scattering matrix of a narrow, resonant, (half-wave) shunt slot in the broad face of an x-band multimode waveguide is determined experimentally and compared with present theory. A high power, (10 watt), traveling-wave tube is used in conjunction with thermistors and power meters for essentially dc measurement of attenuation and phase. Difficulties associated with modulation and crystal detection are discussed.

Appreciation is due Professor R. M. Johnson of the faculty, U. S. Naval Postgraduate School, for technical advice and equipment.

TABLE OF CONTENTS

Chapter		Page
I	INTRODUCTION	1
II	THEORY OF THE SCATTERING MATRIX	3
III	DESCRIPTION AND OPERATION OF EQUIPMENT	11
IV	CALCULATIONS AND RESULTS	25
V	DIFFICULTIES WITH CRYSTAL	39
VI	CONCLUSIONS	48

APPENDICES

A	DATA SHEETS	52-55
B	EQUIPMENT	56
	BIBLIOGRAPHY	57

LIST OF ILLUSTRATIONS

Figure		page
1.	Photograph Of Microwave Bridge Equipment	6
2.	Schematic Of Microwave Bridge	10
3.	Photograph Of Slot In Test Section	15
4.	Photograph Of Power Generating Section	16
5.	Photograph Of Test Section and Measuring ports.	17
6.	Schematic of matching arm section	19
7.	Magic T "β"	20
8.	Magic T "α"	20
9.	Photograph Of Mode Transducer and Slide-Screw-Tuner	21
10.	Graph Of System Phase Variation With Temperature	23
11.	Graph Of System Phase Variation With Time During Warm-up Period	24
12.	Oscilloscope Photographs Of Modulated Crystal Output	40
13.	Graph Of Crystal Output Variation With Variation Of Input Attenuation To Traveling Wave Tube	41
14.	Graph Of Crystal Output With Variation Of Attenuation Of Output Of Traveling Wave Tube	42
15.	Graph Of Crystal Output With Various Combinations Of Two Attenuators	43

CHAPTER I

INTRODUCTION

Measurements of the scattering coefficients of narrow shunt slots at x-band frequencies have received considerable attention/1/, /2/, /3/. It was the intention of this investigator to first verify the work performed by Lary /1/, and then measure the coefficients for several different slots including wide slot radiators.

During the initial stages of verifying Lary's work, a combination of a traveling wave-tube capable of a maximum of two watts and crystal detectors requiring 1000 cycle modulation of the rf. power were used. The nonlinearities of the power measurements obtained in this manner were too unreliable to continue the work and to date they have not been overcome.

The great difficulties experienced with this system will be presented in a later section of this paper.

The procurement of balanced thermistors and power meters which were stable at power levels of one microwatt made it possible to perform the measurements presented here.

It was found that measurements could be obtained which were accurate to within 0.5 degrees and 1.0 db. However, in order to obtain them, extreme care and patience were necessary to insure stabilization of all components.

Many precise corrections were also required to account for the imperfect design of the transducers used to convert TE_{10} to TE_{20} mode propagation; and for the arrangement of the various input and detection ports.

CHAPTER II

THEORY OF THE SCATTERING MATRIX.

An obstacle in a multi-mode wave guide is in effect a multiple terminal pair network coupling the sets of transmission lines which are equivalent to the propagating modes of the waveguide. The coupling network is a four-terminal-pair for a two-mode transmission system such as is investigated in this paper. The relation between the input and output voltages and currents in the equivalent transmission line and network system can be characterized in several equivalent ways; by an impedance matrix, a scattering matrix, or a transmission matrix. These various representations are equivalent, and transformation from one to the other, while tedious, is readily accomplished / 4/ .

The impedance or admittance matrix relates the currents and voltages at the obstacle and has the advantages of being symmetric, that is $Z_{ik} = Z_{k}$; or $Y_{ik} = Y_{ki}$, and of relating directly the field components to the low frequency concepts of lumped constant components; thus, from it one can draw an equivalent circuit using reactances and resistances to represent the discontinuity. Its primary disadvantage is that a shift in reference planes is a cumbersome procedure.

The scattering matrix relates the incident and reflected (scattered) wave amplitudes of the discontinuity.

It also has the advantage of being symmetric but the equivalent circuit concept is lost to some extent. On the other hand, a shift in reference planes is almost trivial and coupling coefficients are easily obtained.

As an illustration of the method for assembling a scattering matrix, consider a four-terminal-pair obstacle coupling two sets of transmission lines (in our case TE_{10} and TE_{20}). Note that these results can be extended to n-pair terminal structures as well. The obstacle is considered to be linear and bi-lateral. It is also assumed that the lines are terminated in their respective characteristic impedances and that the input devices are perfectly matched to their respective lines and that there is no cross coupling at their end.

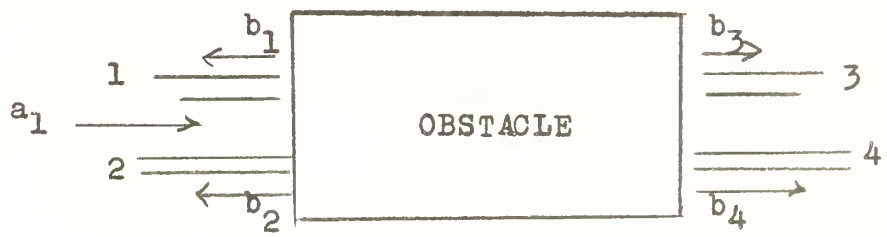

If voltage wave a_1 is sent into terminal 1, then amplitude b_1 will be reflected and b_2, b_3, b_4, will emerge from terminals 2, 3, and 4, respectively. There will be no secondary reflections into terminals 2, 3, and 4, from their respective transmission lines, provided they are properly terminated and do not couple to one another.

If incident waves a_2, a_3, and a_4 are sent in turn into the other terminals of the obstacle one can write:

$$b_1 = S_{11}\, a_1 + S_{12}\, a_2 + S_{13}\, a_3 + S_{14}\, a_4$$

$$b_2 = S_{21}\, a_1 + S_{22}\, a_2 + S_{23}\, a_3 + S_{24}\, a_4$$

$$b_3 = S_{31}\, a_1 + S_{32}\, a_2 + S_{33}\, a_3 + S_{34}\, a_4$$

$$b_4 = S_{41}\, a_1 + S_{42}\, a_2 + S_{43}\, a_3 + S_{44}\, a_4$$

If, as assumed, the obstacle is linear and bilateral, then reciprocity holds and the matrix will be symmetric:

$$S_{ki} = S_{ik}$$

We can also re-write the above equations as:

$$\begin{bmatrix} b_1 \\ b_2 \\ b_3 \\ b_4 \end{bmatrix} = \begin{bmatrix} S_{11} & S_{12} & S_{13} & S_{14} \\ S_{21} & S_{22} & S_{23} & S_{24} \\ S_{31} & S_{32} & S_{33} & S_{34} \\ S_{41} & S_{42} & S_{43} & S_{44} \end{bmatrix} \begin{bmatrix} a_1 \\ a_2 \\ a_3 \\ a_4 \end{bmatrix}$$

thus illustrating the "scattering matrix".

The transformations from the scattering matrix to the impedance matrix is given in the literature [4].

For this investigation:

$a_1 = a_3 =$ TE_{10} incident

$a_2 = a_4 =$ TE_{20} incident

$b_1 = b_3 =$ TE_{10} reflected

$b_2 = b_4 =$ TE_{20} reflected

Due to the bilateral properties of the slot it was only necessary to measure the first two rows of the matrix.

The coefficients were measured in the following manner:

S_{11}: The TE_{10} mode signal reflected with TE_{10} mode incident.

S_{12}: The TE_{10} mode signal reflected with TE_{20} mode incident.

S_{13}: The TE_{10} mode signal transmitted with TE_{10} mode incident.

S_{14}: The TE_{10} mode signal transmitted with TE_{20} mode incident.

S_{21}: The TE_{20} mode signal reflected with TE_{10} mode incident.

S_{22}: The TE_{20} mode signal reflected with TE_{20} mode incident.

S_{23}: The TE_{20} mode signal transmitted with TE_{10} mode incident.

S_{24}: The TE_{20} mode signal transmitted with TE_{20}

mode incident.

Due to the principle of continuity of fields and assuming normalization of both modes,

$$S_{11} + S_{13} = S_{22} + S_{24} = 1.0 \angle 0^\circ$$

Also, due to symmetry,

$$S_{12} = S_{21} = S_{14} = S_{23}$$

Held, [2], using an integral equation method, developed an analytical expression for the scattering coefficients as follows:

$$S_{iK} = \frac{\frac{4\pi}{ab}\sqrt{\frac{K}{\beta_i \beta_K (K^2-\beta_i^2)(K^2-\beta_K^2)}}\cos\frac{K\pi x}{a}}{\left[D_i(2\pi) - \frac{4\pi}{ab}\sum_{V=1}^{N'} \frac{K\cos^2\frac{2\pi x}{a}}{\beta_V (K^2-\beta_V^2)} \cos^2\frac{\beta_V \pi}{K2}\right]}$$

$$j\,\frac{\cos\frac{2\pi x}{a}\cos\beta_i \ell \cos\beta_K \ell}{\left[S_i(2\pi) - \frac{2\pi}{ab}\sum_{V=1}^{N} \frac{K\cos^2\frac{V\pi x}{a}}{\beta_V (K^2-\beta_V^2)} \sin\frac{\beta_V}{K}\pi\right]}$$

where for our case with f = 9,375 mc:

a = wide dimension of waveguide = 4.064 cm
b = narrow dimension of guide = 1.016 cm
λ = 3.2 cm
x = distance from edge of guide to slot = 0

$$\frac{2m\pi x}{a} = 1.0$$

$$K = \frac{2\pi}{\lambda} = 1.962 \text{ cm}^{-1}$$

$$1 = \frac{2\pi}{\lambda_{g_1}} = 1.21 \text{ cm}^{-1}$$

$$2 = \frac{2\pi}{\lambda_{g_2}} = 1.21 \text{ cm}^{-1}$$

And thus:

$$S_{mn} = \frac{4\pi}{ab}(0.576 + j.093) \frac{K \cos(\frac{\beta_m}{k} 90^0)(\cos \frac{\beta_n}{k} 90^0)}{\beta_m \beta_n (k^2 - \frac{2}{n})(k^2 - \beta_m^2)}$$

and in accordance with the definitions of each coefficient given above:

$$S_{11} = \frac{4\pi}{4.13} K \frac{(.576 + j.093)}{\beta_1 (k^2 \quad \frac{2}{1})} \cos^2(\frac{\beta_1}{k} 90^0)$$

$$S_{11} = .0498 + j.008$$

and

$$S_{21} = \frac{4\pi}{4.13} \frac{k(0.576 + j.093)}{\sqrt{\beta_1 \beta_2 (k^2 - \beta_1^2)(k^2 \beta_2^2)}} \cos(\frac{1}{k} 90^0) \cos(\frac{\beta_2}{k} 90^0)$$

$$S_{21} = .138 + j.022 = S_{12} = S_{14} = S_{23}$$

$$S_{22} = \frac{4\pi}{4.13} \frac{K(.576 + j.093) \cos^2(\frac{\beta_2}{k} 90^0)}{2(k^2 - \beta_2^2)}$$

$$S_{22} = .382 + j.062$$

These theoretical results are compared with the experimental data at the end of this paper.

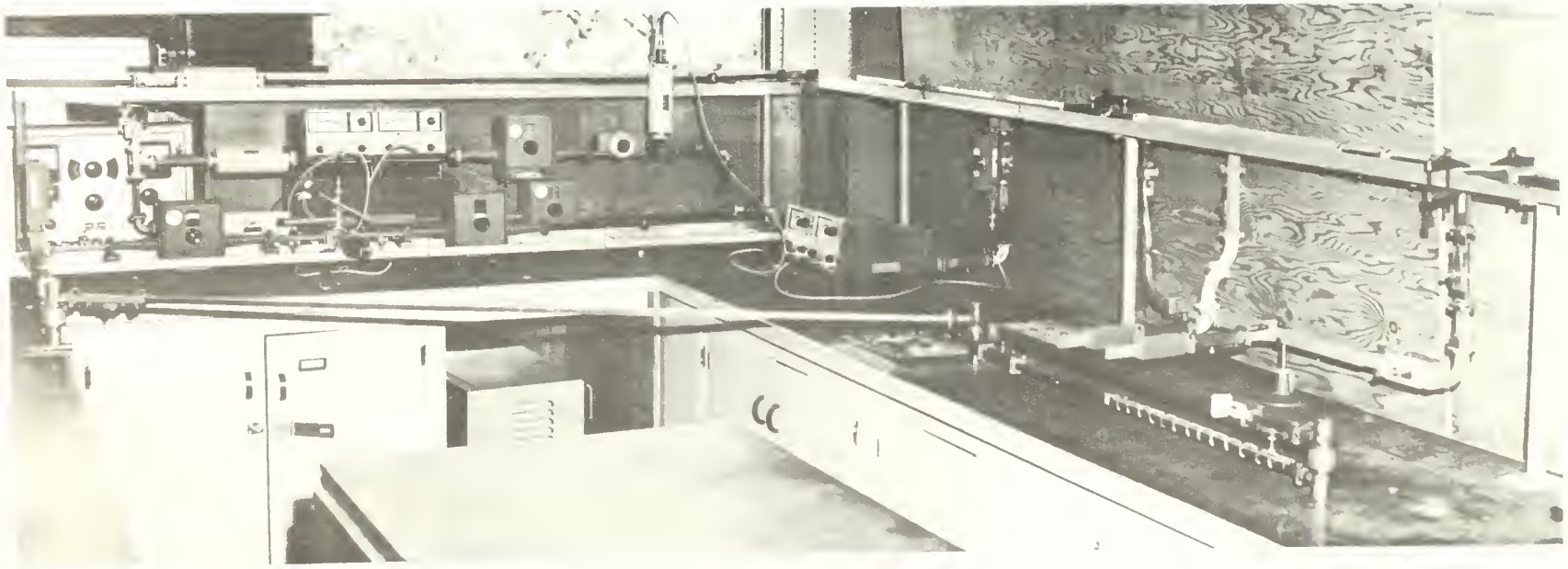

Overall view of microwave bridge. [illegible] and [illegible]orlitide measuring equipment [illegible] in center with [illegible] right and test section on far right [illegible] partly closing.

Fig. 1

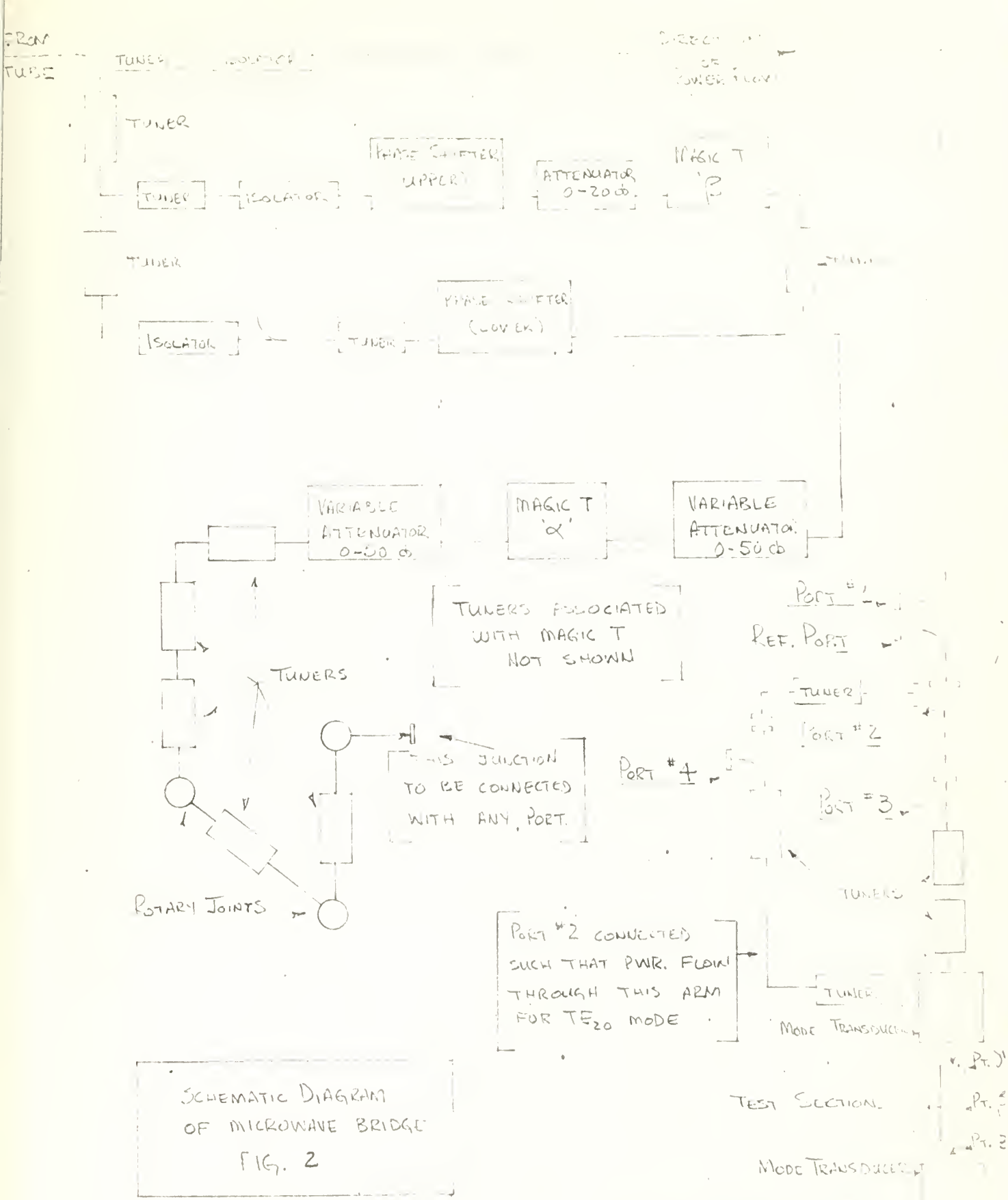

SCHEMATIC DIAGRAM
OF MICROWAVE BRIDGE
FIG. 2

CHAPTER III

DESCRIPTION AND OPERATION OF EQUIPMENT.

The microwave bridge, shown in Figs. 1 and 2, operates on the principle of comparing the signal from one of the ports numbered one through six, or the Ref. port, with a signal direct from the traveling wave tube. This comparison takes place at magic T "α". The section of waveguide connected with rotary joints is the common arm used to connect one side of magic T "α" to each of the ports of interest. The magnitude and phase of the signal direct from the traveling wave tube, called the reference signal, is varied by the lower phase shifter and the attenuator as shown. An attenuator is also required in the arm with the rotary joints in order to reduce signals from the numbered ports which are greater than the reference signal. Attenuation introduced on the rotary joint side of magic T "α" was labeled positive and attenuation introduced by the attenuator on the phase shift side of the magic T was labeled negative. When the phase and magnitude of the reference signal was adjusted to be exactly equal to that coming through the arm with the rotary joints, a null of better than 60 db down from the original incident power was measured at port 3 of magic T "α". (see Fig. 8). The upper phase shifter was introduced for the following purpose: The lower phase shifter did not remain matched with variations of phase; thus it was nec-

essary to re-adjust the slide-screw tuner, shown immediately preceding the lower phase shifter, each time this phase shifter was changed. In doing so, the original phase reference was lost. But by adjusting the upper phase shifter to coincide with the resultant signal coming out of the lower phase shifter, a second order approximation to the actual phase of the signal entering magic T "α" could be obtained. The upper phase shifter was brought into coincidence with the signal entering magic T "α" by adjusting it until a null was obtained at port 2 of magic T"β", (see Fig. 7).

The 0-20 db attenuator shown between the upper phase shifter and magic T "β" was adjusted to match the magnitudes of the two signals into magic T "β". Since the amplitudes of the two signals were constant with variations in the phase shifters, and the small variation in the slide screw tuner, only one adjustment of this variable attenuator was necessary.

Port #1 was used to monitor the amplitude of the phase incident on the bridge. This was necessary as it was found that the phase reference of the system stabilized only after at least two hours of operation. For this reason the input attenuator to the tube was used to reduce the r.f. power while changing system components rather than turning off the high voltage to the traveling-wave tube.

Port #2 was used only as a junction. When this port was connected to the arm containing port #4, r.f. power was directed to the transducer such that the TE_{20} mode was incident in the test section. On the other hand, when port #2 was connected to the arm containing port #3, TE_{10} power was incident on the test section. Matched loads were connected to the end of whichever arm was not being used in the above connections.

Port #3 was used to measure all TE_{10} mode signals reflected from the test section.

Port #4 was used to measure all TE_{20} mode signals reflected from the test section.

Port #5 was used to measure all the TE_{20} mode signals transmitted through the test section.

Port #6 was used to measure all the TE_{10} mode signals transmitted through the test section.

The Ref. port was used to measure both the TE_{10} and TE_{20} mode signals that were reflected from the test section. This port was essential in order to determine the difference in phase and amplitude of the two modes reflected from a short located at point γ (the beginning of the test section), and thus obtain a comparison of the phase and amplitudes of the two different modes incident on the test section. As will be pointed out later, it was essential that these corrections be known as the accuracy of the scattering matrix depended on both incident

signals being precisely the same.

The Ref. port was also valuable in providing a check on measurements such as the difference in phase and amplitude between a signal reflected from a short at port #6, and a signal reflected from a short located at point Z (the end of the test section), since this could be measured at port #3 as well as the Ref. port. The Ref. port provided a similar check on measurements taken at port #4 for shorts at port #5 and point Z. The close agreement of these measurements, as shown below, are indicative of the degree of accuracy attainable with this microwave bridge.

Port #3 -	1.015	$\angle 21.20^\circ$	Difference in signal reflected from a short at port #6 and point Z.
Ref. port -	1.021	$\angle 20.0^\circ$	

Port #4 -	1.051	$\angle 155.3^\circ$	Difference in signal reflected from a short at port #5 and point Z.
Ref. port -	1.035	$\angle 155.0^\circ$	

The mode transducers which converted the TE_{10} mode to TE_{20} mode and vice versa and the special magic T "$\propto$", were manufactured by the University of California, Berkeley, and are shown in Fig's 1 and 9. The slide screw tuner shown in Fig. 9 was manufactured at the U. S. Naval Postgraduate School. Two additional views of the equipment are presented in Fig's 4 and 5.

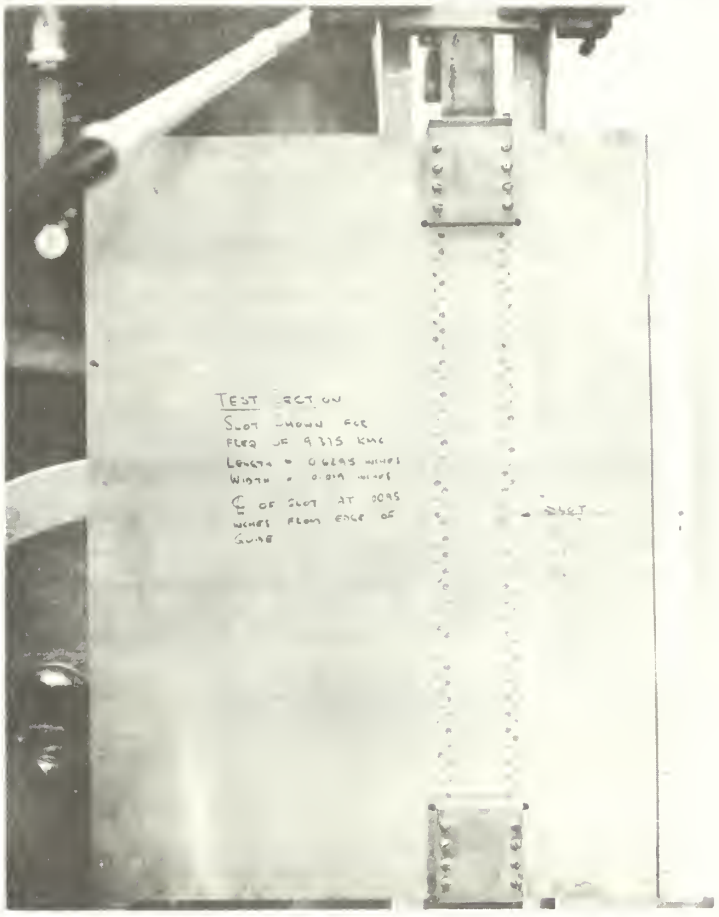

infinite ground plane.

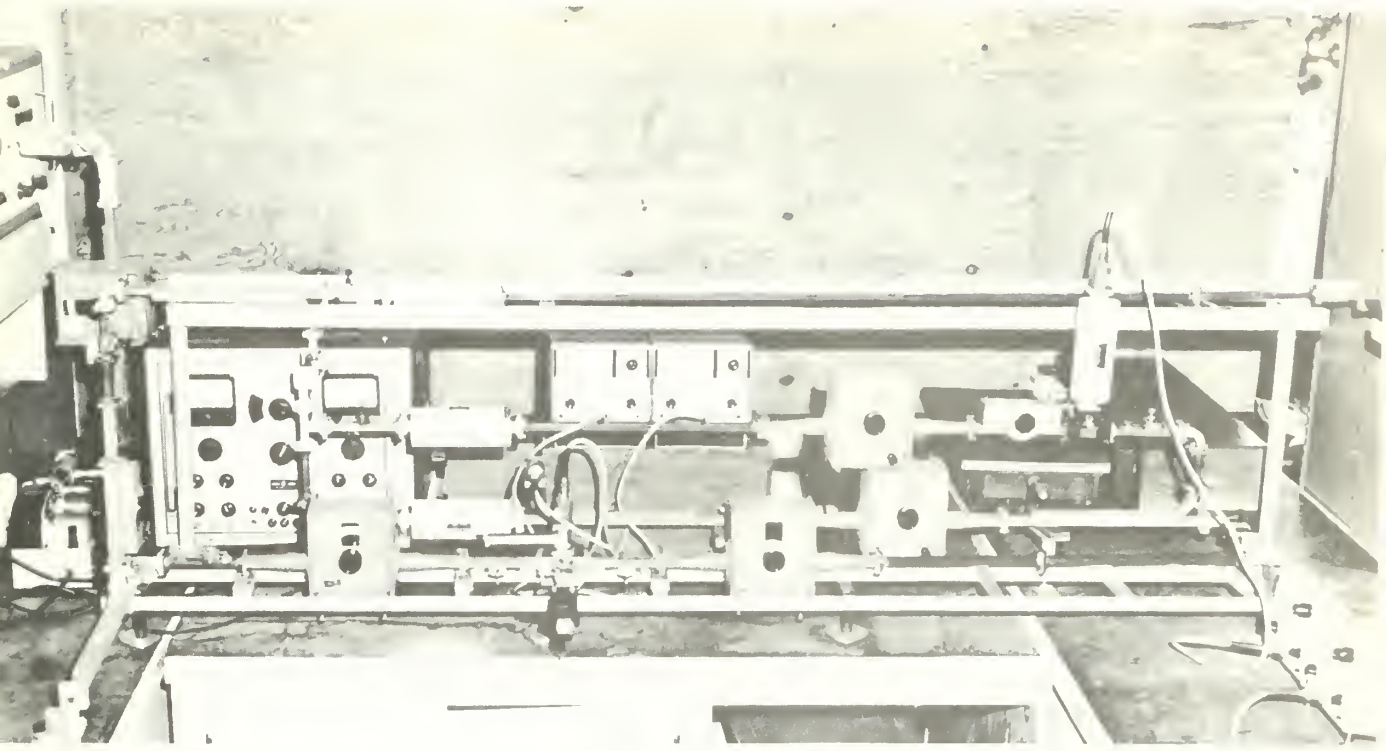

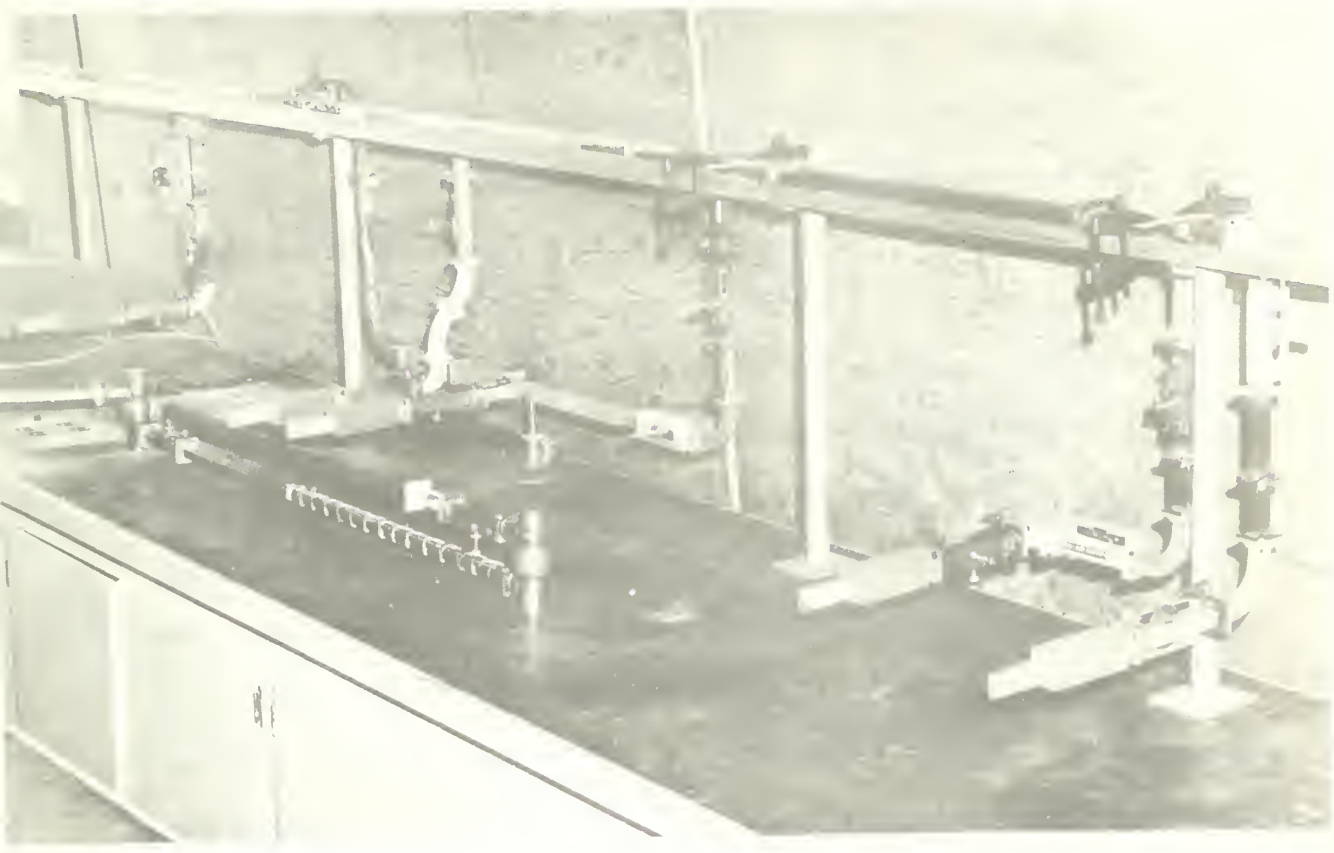

The slot, shown in Fig. 3, was cut in a 24 inch square sheet of .05 inch thick brass. The slot was .6295 inches long ($\lambda/2$ for 9,375 mc). It was .019 inches wide and was located on the exact edge of the broad wall of the guide. In other words the centerline of the slot was .0095 inches from the edge of the guide.

The matching arm shown in Fig. 6 was constructed first. The directivity signal of the 10 db reverse coupler in the matching arm was then matched out by connecting a sliding load to the slide-screw tuner shown, and then adjusting this tuner until the variation in the reflected signal with movement of the sliding load was less than one db. Note that this could not be accomplished when a crystal detector was used as will be discussed later. Thermistors and power meters were used throughout the actual operation of the microwave bridge.

Having tuned out the directivity signal in the matching arm 10 db coupler, the high-power terminations were matched to have a reflection greater than 55 db down from the incident power level. The best of these loads, with a match of 63 db, was subsequently used as the termination for all the waveguide sections, transducers and directional couplers that required matching. Matching T "β" was matched as follows:

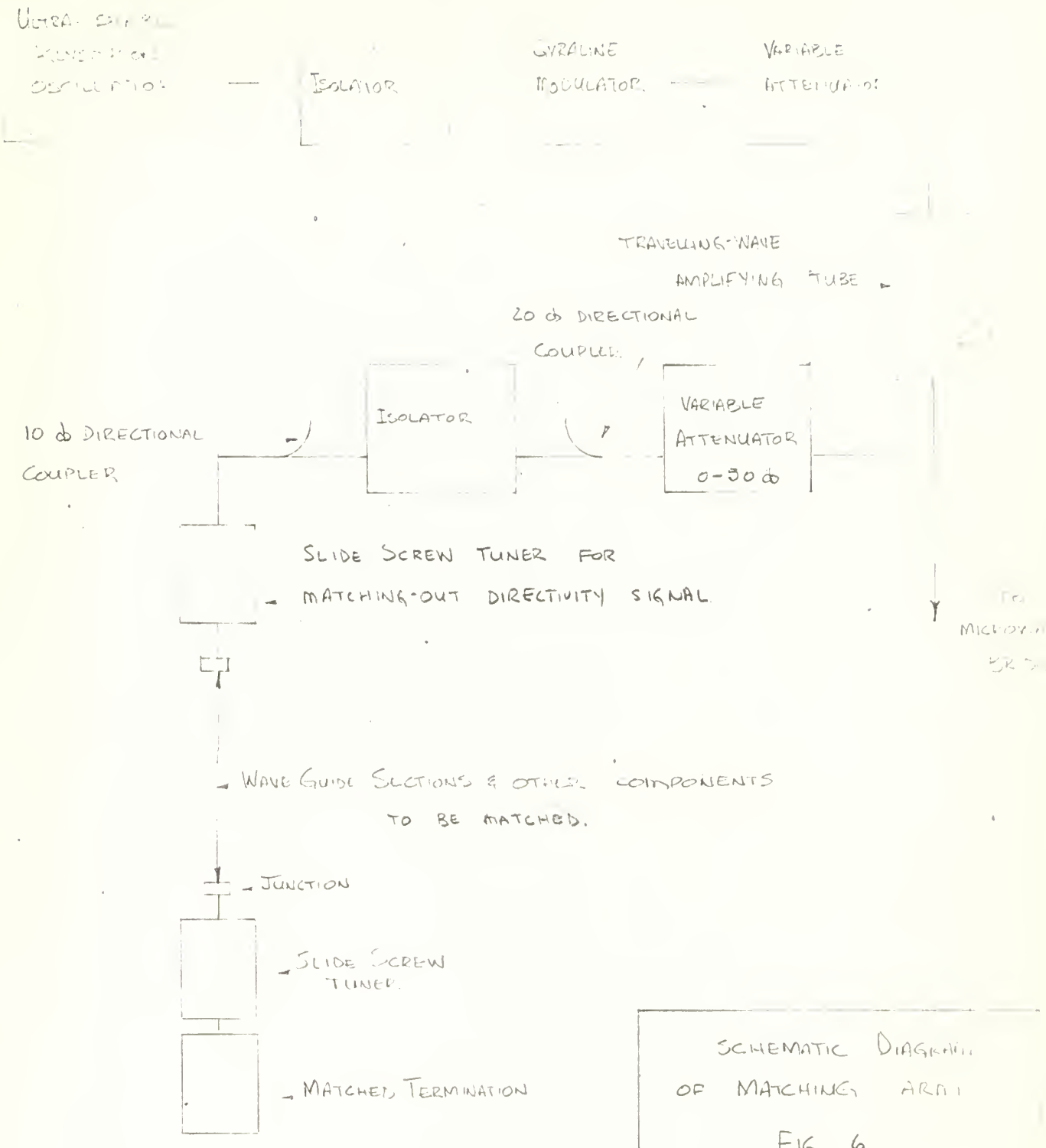

SCHEMATIC DIAGRAM OF MATCHING ARM

FIG. 6

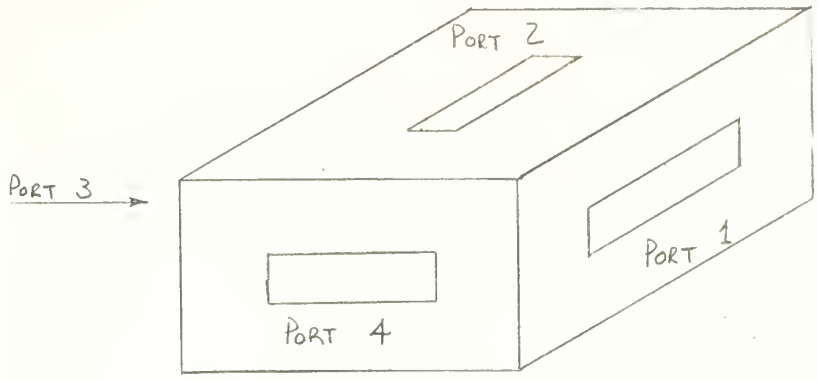

MAGIC T "β"

FIG. 7

With a matched load fixed to port 4, and an isolator on port 2, isloation between ports 1 and 3 was 47 db.

Magic T "α" was matched as follows:

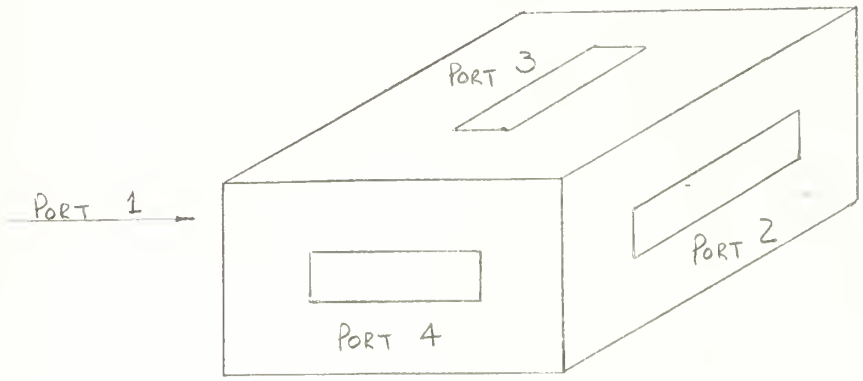

MAGIC T "α"

FIG. 8

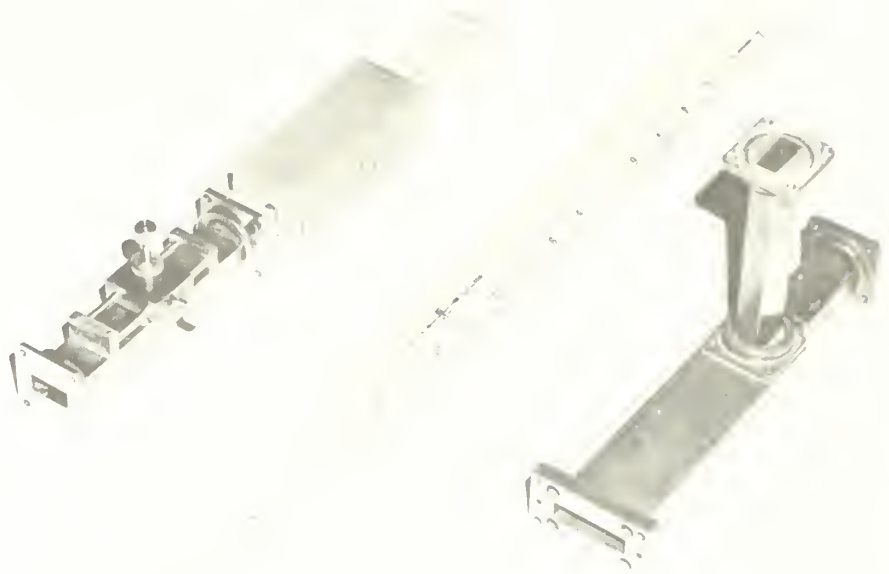

Note: A matched load was fixed on port 4 throughout.

a) With matched loads on 1 and 2 and input in 3, the reflection was 44 db down from the incident signal.

b) With input in 2, the output at 3 was down 56 db.

c) With the input in 3, the output from 2 or 1 was down 61.0 db.

d) With the input in 3 and matched loads at 1 and 2, the reflection was down 47 db.

In the course of the investigation it was found that the phase of the system increased approximately 25.0 degrees during a two hour warming-up period after the r.f. power was applied. It was also found that the phase decreased approximately 2.4 degrees centigrade per degree increase in the ambient temperature. Since these two trends were not consistent, the increase of phase with warm-up time was not fully explained. Figure 10 presents a plot of phase variation with temperature and Fig. 11 is a plot of the phase increase with time. Note that in Fig. 11 the excursions of the ambient temperature are superimposed and their effect on the rate of drift with time can be seen. The first page of the data shows the temperature corrections that were applied. Measurements for both modes were first taken with a two-mode section of wave-guide in the 24 inch test section and then with the slot inserted. Several readings were also taken with

a short at points Y, (beginning of test section) Z (end of test section), and ports #5 and #6.

Exhaustive tests of each of the above were repeated on five separate occasions.

As can be seen in the data in Appendix A, the variations in phase observed while repeating the measurements were occasionally as high as three degrees. These could not be corrected in any way so their arithmetic averages were used in selecting the value to be used in the calculations. The data of 16 April were generally considered unreliable because on this occasion the high voltage to the traveling wave tube was removed each time a new measurement was taken, rather than decreasing the r.f. power by means of the attenuator as was done in later measurements. Since the drift of phase with time has not been fully explained except that it was opposite to the drift with increasing ambient temperature, the precise effect on system phase, as a result of removing the high power, could not be quantitatively defined. But, as a result of this phase variation with time following application of high power to the tube, the data of 16 April was not used in the arithmetic averaging process.

The junctions at both ends of the test section had alignment pin holes drilled, but they did not match very precisely. This is one area that could be improved on to reduce the phase variation between repeated measurements.

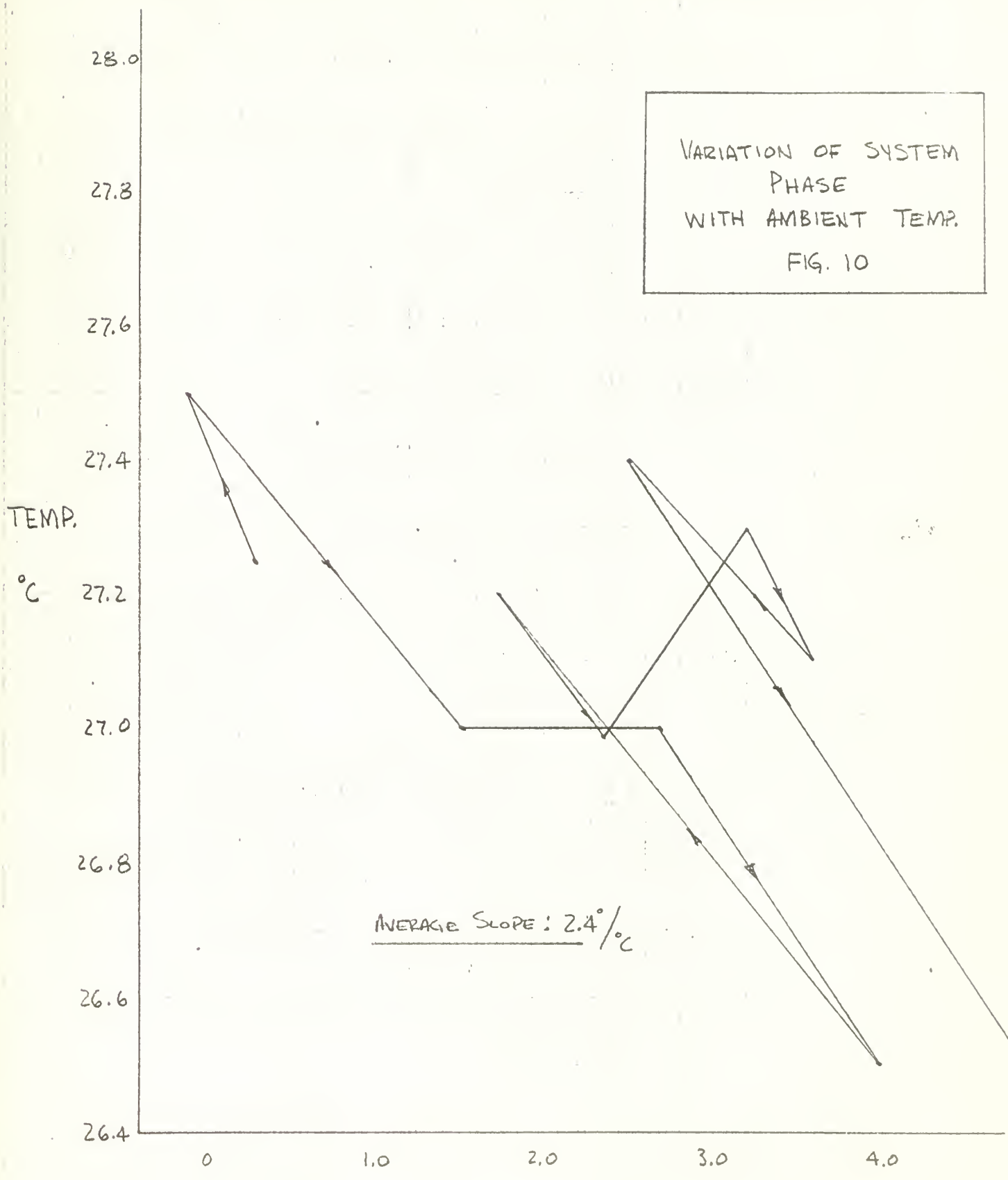
VARIATION OF SYSTEM PHASE WITH AMBIENT TEMP.
FIG. 10
28.0
27.8
27.6
27.4
27.2
27.0
26.8
26.6
26.4
TEMP. °C
AVERAGE SLOPE : 2.4°/°C
0
1.0
2.0
3.0
4.0
PHASE - DEGREES.

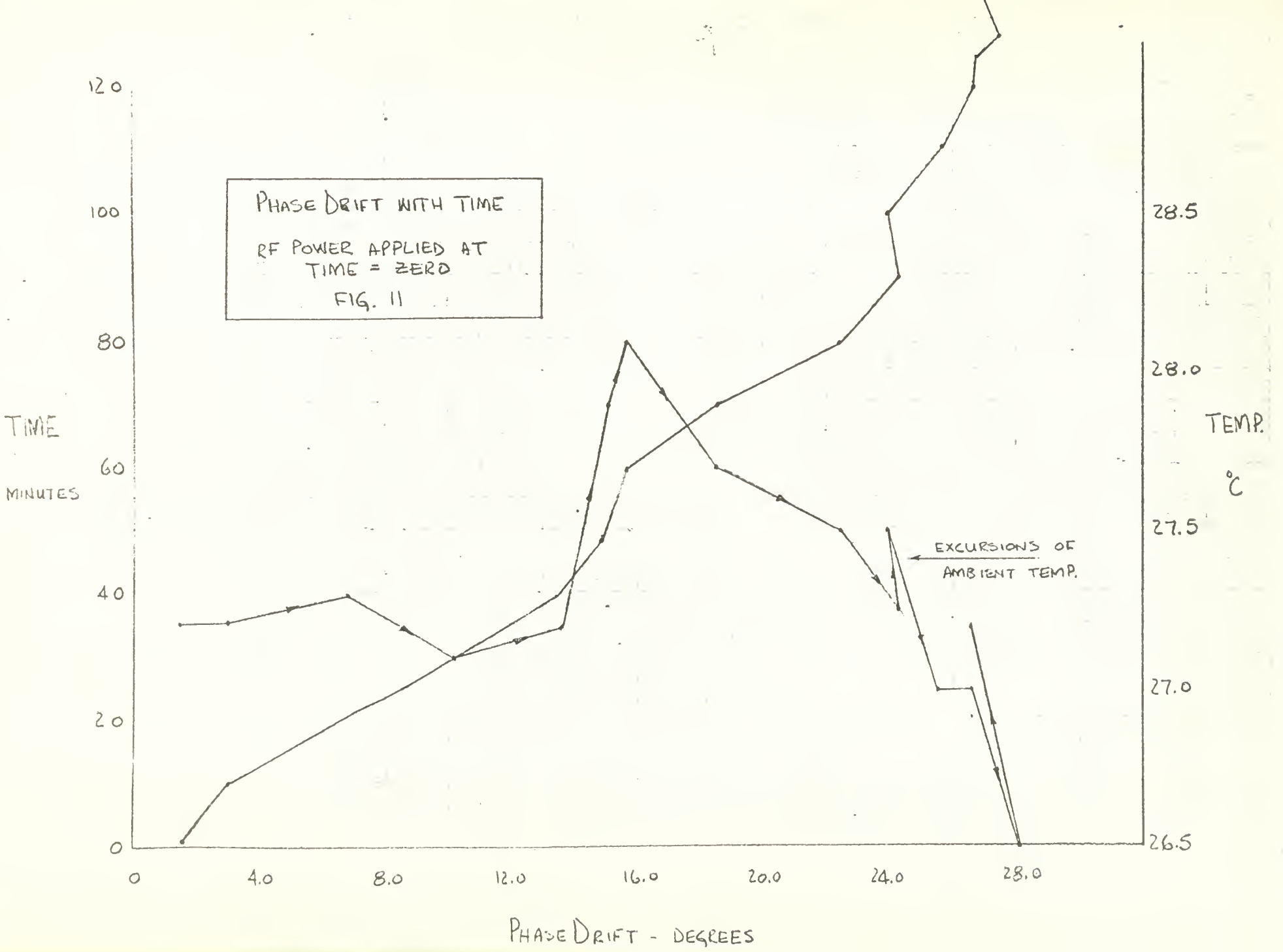
PHASE DRIFT WITH TIME
RF POWER APPLIED AT TIME = ZERO
FIG. 11
TIME
MINUTES
120
100
80
60
40
20
0
TEMP.
°C
28.5
28.0
27.5
27.0
26.5
EXCURSIONS OF AMBIENT TEMP.
0
4.0
8.0
12.0
16.0
20.0
24.0
28.0
PHASE DRIFT - DEGREES

CHAPTER IV

CALCULATIONS AND RESULTS

In the calculations which follow the following symbolism will be used:

3_{10}guide — meaning the signal measured at port #3 when TE_{10} mode was incident on the test section and the two mode waveguide was in the test section.

$4_{20}\gamma'$ — meaning the signal measured at port #4 when TE_{20} mode power was incident on the test section and there was a short at point γ' (the beginning of the test section).

Ref_{10_6} — meaning the signal measured at the Ref. port when TE_{10} power was incident on the test section and there was a short at port #6.

Note that in all cases when shorts were applied at points Z, and γ' and ports #5 and #6, the guide was in the test section.

4_{20}slot — meaning the signal measured at port #4 when TE_{20} mode power was incident and the slot was in the test section.

The computation of the phase and attenuation change between a signal at port #6 and the center of the test section, (γ), was done by two methods:

a) Using data obtained from port #3.

b) Using data obtained from Ref. port.

By Method (a)

$$\frac{\#3_{10_Z}}{\#3_{10_6}} = \frac{11.6 \angle 259.0}{11.23 \text{ db} \angle 182.0} = .37 \text{ db} \angle 77.0$$

$$= 1.042 \angle 77.0^\circ$$

$$\frac{\#3_{10}}{\#3_{10_Z}} = \frac{11.7 \text{ db} \angle 281.0}{11.6 \text{ db} \angle 259.8^\circ}$$

$$= 0.1 \text{ db} \angle 21.2^\circ = 1.015 \angle 21.0^\circ$$

The above two values are the difference in phase and amplitude of a TE_{10} mode signal reflected from point Z and port #6, and point and point Z; respectively. Before proceeding further we compared these results with those obtained by method (b):

$$\frac{\text{Ref}_{10_Z}}{\text{Ref}_{10_6}} = \frac{10.9 \text{ db} \angle 327.0}{10.42 \text{ db} \angle 248.0}$$

$$= .48 \text{ db} \angle 79.0^\circ$$

$$= 1.054 \angle 79.0^\circ \neq 1.042 \angle 77.0^\circ$$

Average of the two methods for $(6 \longrightarrow Z)_{10}$ $= 1.048 \angle 78.0^\circ = .41 \text{ db} \angle 78.0$

$$\frac{\text{Ref}_{10_\gamma}}{\text{Ref}_{10_Z}} = \frac{11.1 \text{ db} \angle 347.0}{10.9 \text{ db} \angle 327.0}$$

$$= 0.2 \text{ db} \angle 20.0^\circ$$

$$= 1.021 \angle 20.0 \neq 1.015 \angle 21.2^\circ$$

Average of the two methods for $(Z \longrightarrow \gamma)_{10}$ $= 1.018 \angle 20.6^\circ = .163 \text{ db} \angle 20.6^\circ$

The above corrections are for two-way reflections, but we need the correction for one-way travel between port 6 and point β. To obtain this we must first obtain the one-way correction between point Z and point β. Since we want the correction for one-way travel over one half of the distance from Z to γ, and the data is for a two-way reflection over the entire distance, we have:

$$TE_{10}(Z \rightarrow \beta) = (Z \rightarrow \beta)_{1\ way_{10}} = \frac{1}{4}\left(\frac{{}^{3}10_{\gamma}}{{}^{3}10_{Z}}\right)$$

$$= 1.0045 \angle 5.15$$

We must also take one half of the data given for the correction from 6 to Z in order to have one way travel: Now correction from #6 to is:

$$(6 \rightarrow Z)_{10}(Z \rightarrow \beta)_{10} = (1.024 \angle 39.0^{\circ})(1.0045 \angle 5.15^{\circ})$$

$$(6 \rightarrow \beta)_{10} = 1.028 \angle 44.15^{\circ}$$

Note: in the following calculations the following corrections will be used,

$$(\gamma \rightarrow \beta)_{2\ way_{10}} = .991 \angle -10.3^{\circ}$$

$$(\beta \rightarrow \gamma)_{1\ way_{10}} = 1.0045 \angle +5.15^{\circ}$$

Computing the correction from Port #5 to β is done similarly:

$$\frac{{}^{4}20_{\gamma}}{{}^{4}20_{Z}} = \frac{11.8 \text{ db} \angle 345.4^{\circ}}{11.36 \text{ db} \angle 190.1^{\circ}}$$

$$= .44 \text{ db} \angle 155.3^{\circ}$$

$$= 1.051 \angle 155.3^{\circ}$$

$$\frac{{}^{4}20_{Z}}{{}^{4}20_{5}} = \frac{11.36 \angle 190.1}{11.08 \angle 285.1}$$

$$= 0.28 \text{ db } \angle -95.0$$

$$= 1.03 \angle -95.0^{\circ}$$

$$\frac{\text{Ref}_{20}}{\text{Ref}_{20_{Z}}} = \frac{10.7 \text{ db } \angle 301.0}{10.4 \text{ db } \angle 146.0} = .3 \text{ db } \angle 155.0$$

$$= 1.035 \angle 155.0 \neq 1.051 \angle 155.3^{\circ}$$

Average of two methods $(Z \rightarrow f)_{2way_{20}} = \underline{1.04 \angle 155.15^{\circ}}$

$$\frac{\text{Ref}_{20_{Z}}}{\text{Ref}_{20_{5}}} = \frac{10.40 \text{ db } \angle 142.0}{9.97 \text{ db } \angle 239.5}$$

$$= 0.43 \text{ db } \angle -97.5^{\circ}$$

$$= 1.05 \angle -97.5 \neq 1.03 \angle -95.0^{\circ}$$

Average of two methods $(5 \rightarrow Z)_{2way_{20}} = \underline{1.04 \angle -96.0^{\circ}}$

Similarly, the calculation for the correction from #5 to f is as follows:

TE_{20} $(Z \rightarrow \beta) = \frac{1}{4}(1.04 \angle 155.15^{\circ}) = 1.01 \angle 38.93^{\circ}$

TE_{20} $(5 \rightarrow Z) = \frac{1}{2}(1.04 \angle -96.0^{\circ}) = 1.02 \angle -48.0^{\circ}$

TE_{20} $(5 \rightarrow \beta) = (1.02 \angle -48.0^{\circ})(1.01 \angle 38.93^{\circ}) = 1.03 \angle -9.07^{\circ}$

In addition note:

$$(\gamma \rightarrow \beta)_{2way_{20}} = .98 \angle -77.37^{\circ}$$

$$(\beta \rightarrow \gamma)_{1\ way_{20}} = 1.01 \angle 38.93^{\circ}$$

In order to compare the reflected signals at Ports 3 and 4 with the incident power which generated them, it was necessary to do the following:

a) Place a short circuit at point γ.

b) Measure the reflected signal at port #3 for TE_{10}; at port #4 for TE_{20}; and at the Ref. port for both TE_{10} and TE_{20}.

Then, as an example, the TE_{20} mode signal, reflected from the slot when TE_{10} mode was incident, was detected at port #4 and compared with the TE_{20} signal reflected from the short. Now note that in the above case TE_{10} power is actually incident on the slot but the reflected signal must be compared with the reflection from the short with TE_{20} incident. Since the two arms used to feed TE_{20} and TE_{10} to the test section do not have the same trans-

mission coefficients, the signals from the short must be corrected by the amount of this difference.

For the example above, this correction would be:

$$4_{20_{\gamma'}}\left(\frac{\text{Ref}_{10_{\gamma'}}}{\text{Ref}_{20_{\gamma'}}}\right)\left(\frac{1}{2}\right)$$

In addition, since the short was located at point γ' and not point β, it was necessary to correct the reference signal by $(\gamma' \rightarrow \beta)_{2\ \text{way}_{20}}$ (meaning the phase and amplitude difference in a TE_{20} signal after 2 way travel from γ' to β). Thus the total correction would be:

$$4_{20_{\gamma'}}\left(\frac{\text{Ref}_{20}}{\text{Ref}_{20}}\right)\left(\frac{1}{2}\right)(\gamma' \rightarrow \beta)_{2\ \text{way}_{20}}$$

$$=(11.8\ \text{db}\ \angle 345.4^{\circ})\left(\frac{11.1\ \text{db}\ \angle 347.0^{\circ}}{10.65\ \text{db}\ \angle 301.0^{\circ}}\right)\left(\frac{1}{2}\right)(.98\ \angle -77.87^{\circ})$$

Note also that only one half of the correction $\left(\frac{\text{Ref}_{10_{\gamma'}}}{\text{Ref}_{20_{\gamma'}}}\right)$, is applied. This is so because we are interested in correcting only the signal incident on the short, whereas this correction is the ratio of the reflected signals which have traveled the length of the two arms twice.

Each of the scattering coefficients will now be computed using the data shown in Table I.

$$S_{11} = \frac{3_{10_{\text{slot}}} - 3_{10_{\text{guide}}}}{(3_{10_{\gamma'}} - 180^{\circ})(\gamma' \rightarrow \beta)_{2\text{way}_{10}}}$$

Note that the $3_{10\ guide}$ term would normally be zero if there was no directivity signal in the 10 db coupler used to obtain the reflected signal and there were no reflections from the terminations and the magic T: In this project this signal was greater than -65 db down from the incident signal so was neglected. Note that the directivity of the coupler was only about 45 db so the reflections from the terminations and joints apparently cancelled the directivity.

In the denominator 180° was subtracted from the signal reflected from the short as it was 180° out of phase with the actual incident power.

Thus:

$$S_{11} = \frac{-18.3 \text{ db } \angle 71.4^{\circ}}{(11.8 \text{ db } \angle 281.0^{\circ} - 180^{\circ})(.991 \angle -10.3^{\circ})}$$

$$S_{11} = \frac{.122 \angle 71.4^{\circ}}{3.86 \angle 90.7}$$

$$S_{11} = .0320 \angle -17.3^{\circ}$$

$$S_{11} = .0304 - j.0094$$

$$S_{11} = -29.9 \text{ db } \angle -17.3^{\circ}$$

To compute S_{12}

$$S_{12} = \frac{3_{20_{slot}} - 3_{20_{guide}}}{(3_{10_{\gamma}} - 180^{\circ})(\gamma - \beta)_{1\ way_{20}}} (\beta - \gamma)_{1\ way_{10}} \frac{1}{2}\left(\frac{Ref_{20_{\gamma}}}{Ref_{10_{\gamma}}}\right)$$

Note that again in the numerator it is necessary to subtract the effect of the directivity signal in the coupler and the other reflections in the system. In this TE_{20} mode this signal is significant.

In the denominator it was necessary to apply a correction from $(\gamma - \beta)$ for TE_{20} as this is the incident power, but then from $(\beta - \gamma)$ the correction is for TE_{10} power, the reflected signal being measured.

Thus:

$$S_{12} = \frac{-9.6 \text{ db } \angle 5.0^\circ - 21.0 \text{ db } \angle 80.0^\circ}{(11.8\text{db } \angle 281.0-180)(.9955 \angle -5.15)(.99 \angle -38.9)\frac{1}{2}\left(\frac{10.65\text{db } \angle 301^\circ}{11.1\text{db } \angle 347^\circ}\right)}$$

$$= \frac{(.33 + j.029) - (-.037 - j.081)}{3.855 \angle 34.0^\circ}$$

$$= \frac{.367 + j.11}{3.855 \angle 34.0^\circ} = \frac{.383 \angle 16.7^\circ}{3.855 \angle 34.0^\circ} = .098 \angle -17.3^\circ$$

$$= .0935 - j.0292 = -20.2 \text{ db } \angle -17.3^\circ$$

Computing S_{13}

$$S_{13} = \frac{6_{10}\text{slot}}{6_{10}\text{guide}}$$

There are no corrections necessary in obtaining this coefficient

$$S_{13} = \frac{21.6 \text{ db } \angle 151.0^\circ}{21.9 \text{ db } \angle 150.0} = -.3 \text{ db } \angle 1.0^\circ = .966 + j.0171$$

Computing S_{14}

$$S_{14} = \frac{(6_{20_{slot}} - 6_{20_{guide}})(6 \rightarrow \beta)_{10}}{(5_{20_{guide}})(5 \rightarrow \beta)}$$

For this coefficient, it was necessary to compare the TE_{10} mode transmitted by the slot with the TE_{20} incident signal. Thus the TE_{10} mode measured at port #6 was corrected back to the center of the slot, β , and then compared with the TE_{20} signal measured at port #5 when the guide was in the test section and also corrected back to the center of the slot.

$$S_{14} = \left[-75 \text{ db } \angle 256.0^\circ - (-12.6 \text{ db } \angle 283.0^\circ)\ (1.028\ \angle 44.15^\circ) \right] \Big/ (21.7 \text{ db } \angle 144.0^\circ)(1.03\ \angle -9.07^\circ)$$

$$S_{14} = \frac{(.739 \angle 245.4^\circ)(1.028\ \angle 44.15^\circ)}{12.58\ \angle 134.93}$$

$$S_{14} = .0605\ \angle 154.62 - 180^\circ$$

$$S_{14} = -24.3 \text{ db } \angle -25.38^\circ = .0547 - j.0287$$

Computing S_{24}

$$S_{24} = \frac{5_{20_{slot}}}{5_{20_{guide}}} = \frac{19.55 \text{ db} \angle 153.0^\circ}{21.7 \text{ db} \angle 144.0^\circ}$$

$$S_{24} = -2.15 \text{ db} \angle 9.0^\circ = .78 \angle 12^\circ = .771 + j.122$$

Computing S_{21}

$$S_{21} = \frac{4_{10_{slot}} - 4_{10_{guide}}}{(4_{20_\gamma} - 180^\circ)(\gamma \longrightarrow \beta\ 10_{1way}} (\beta \longrightarrow \gamma)_{20_{1way}} \left(\frac{1}{2}\right) \left(\frac{Ref_{10_\gamma}}{Ref_{20_\gamma}}\right)$$

$$= \frac{(-9.0 \text{ db} \angle 121.0^\circ - (-29.0 \text{ db} \angle 25.0^\circ)}{(11.8 \angle 345.4 - 180^\circ)(.99 \angle -38.9^\circ)(.9955 \angle -5.15^\circ)} \left(\frac{1}{2}\right)\left(\frac{11.1 \angle 347^\circ}{10.65 \angle 301^\circ}\right)$$

$$= \frac{-.183 + j.304 - (.032 + j.0148)}{(3.90 \angle 165.4)(.985 \angle -44.05^\circ)(1.0215 \angle +23^\circ)}$$

$$= \frac{.360 \angle 126.8^\circ}{3.925 \angle 144.4^\circ}$$

$$S_{21} = -20.61 \text{ db} \angle -17.6^\circ = +.0878 - j.0292$$

Computing S_{22}

$$S_{22} = \frac{4_{20_{slot}} - 4_{20_{guide}}}{(4_{20_\gamma} - 180^\circ)(\gamma \longrightarrow \beta\ 2\ way_{20}}$$

$$S_{22} = \frac{1.1 \text{ db} \angle 71.0^\circ - (0)}{(11.8 \angle 345.5^\circ - 180^\circ)(.98 \angle -77.87^\circ)} = \frac{-1.1 \text{ db} \angle -71.0^\circ}{3.82 \angle 87.63^\circ}$$

$$= -12.7 \text{ db} \angle -16.63^\circ = .232 \angle -16.63$$

$$S_{22} = .223 - j.0855$$

Computing S_{23}

$$S_{23} = \frac{\left(5_{10_{slot}} - 5_{10_{guide}}\right)(5 \rightarrow \beta)}{(6_{10_{guide}})(6 \rightarrow \beta)}$$

$$= \frac{\left[(1.6 \text{ db} \angle 355.0^\circ - (-11.8 \text{ db} \angle 277.0^\circ)\right](1.03 \angle -9.07^\circ)}{(21.9 \text{ db} \angle 148.0)(1.028 \angle 44.15^\circ)}$$

$$= \frac{\left[(1.198 - j.105) - (.024 - j.228)\right](1.03 \angle -9.07^\circ)}{12.79 \angle 194.15^\circ}$$

$$S_{23} = \frac{(1.188 \angle 5.9^\circ)(1.03 \angle -9.07^\circ) - 180^\circ}{12.79 \angle 194.15}$$

$$= -20.4 \text{ db} \angle -17.32^\circ$$

$$S_{23} = .0914 - j.0286$$

Checking: $S_{11} + S_{13} = 1.0 \angle 0^\circ$

$$S_{11} + S_{13} = (.0304 - j.0094) + (.966 + j.0171)$$

$$= .9964 + j.0077$$

$$S_{11} + S_{13} = .997 \angle 0.4^\circ$$

$$S_{22} + S_{24} = 1.0 \angle 0^\circ$$

$$S_{22} + S_{24} = (.223 - j.0855) + (.771 + j.122)$$

$$= .994 + j.036$$

$$S_{22} + S_{24} = .995 \angle 2.04^\circ$$

SUMMARY AND COMPARISON OF RESULTS

Coef-ficient	This investigation	Lary's /1/ Investigation	Theory/2/
S_{11}	-29.9 db $/-17.3^\circ$	-27.32 db $/-6.9^\circ$	-26.1 db $/9.1^\circ$
	$.0304 - j.0094$		$.0498 + j.008$
S_{12}	-20.2 db $/-17.3^\circ$	-19.36 db $/-16.5^\circ$	-17.2 db $/9.1^\circ$
	$.0935 - j.0292$		$.138 + j.022$
S_{13}	$-.30$ db $/1.0^\circ$	$-.42$ db $/0.4^\circ$	$-.44$ db $/0.5^\circ$
	$.966 + j.0171$		$.95 + j.009$
S_{14}	-24.3 db $/-25.38^\circ$	-19.21 db $/-16.5^\circ$	-17.2 db $/9.1^\circ$
	$.0547 - j.0287$		$.138 + j.022$
S_{21}	-20.61db $/-17.6^\circ$	-19.64db $/-17.6^\circ$	-17.2 db $/9.1^\circ$
	$.0878 - j.0292$		$.382 + j.062$
S_{22}	-12.7db $/-16.63^\circ$	-11.42db $/-21.8^\circ$	-8.4 db $/9.1^\circ$
	$.223 - j.0855$		$.382 + j.062$
S_{23}	-20.4db $/-17.32^\circ$	-19.49db $/-14.4^\circ$	-17.2db $/9.1^\circ$
	$.0914 - j.0286$		$.138 + j.022$
S_{24}	-2.15db $/9.0^\circ$	-2.46db $/9.5^\circ$	-4.4 db $/5.9^\circ$
	$.771 + j.122$		$.6 + j.06$
$S_{11}+S_{13}$	$.997 /0.4^\circ$	$.996 /0.1^\circ$	$1.0 /0^\circ$
$S_{22}+S_{24}$	$.995 /2.04^\circ$	$1.005 /1.4^\circ$	$1.0 /0^\circ$

CHAPTER V

DIFFICULTIES WITH CRYSTAL DETECTION AND 1000 CYCLE MODULATION

The primary difficulties with the crystal - modulation combination for measurement of the r.f. power levels centered around five main areas which will be discussed in greater detail later:

a) The shape of the modulation envelope became distorted at low (microwatt) power levels and the measured values of crystal output became errotic. (See Fig. 12).

b) Extreme dips occured in the crystal output over a range of output power of the tube when the attenuator controlling the input to the tube was varied. These dips were not apparent when the output power was measured with a thermistor-power meter combination (see Fig. 13).

c) Crystal outputs of the reflected channel from a matched load exhibited an unexplained jump in reflected power when the output power drom the traveling wave tube was attenuated more than about 20 db. (See Fig. 14).

d) The output of the crystals indicated excessive (3 db) non-linearities in the power attenuators which were not apparent when the same attenuators were used in conjunction with thermistor and power meters. (See Fig. 15).

e) It was often impossible to obtain agreement between the Hewlett Packard 415 B Standing Wave Detector and the Hewlett Packard 416 A Ratio Detector for particular mea-

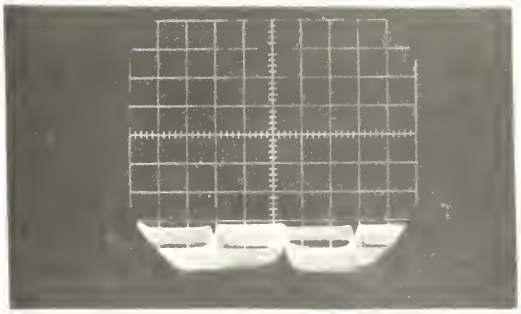

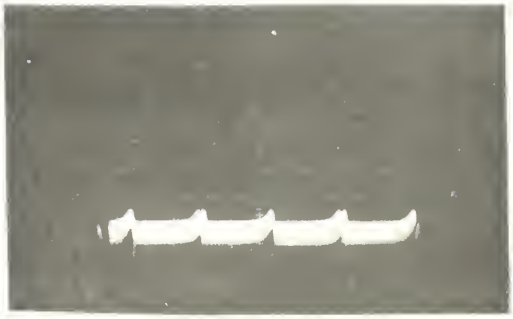

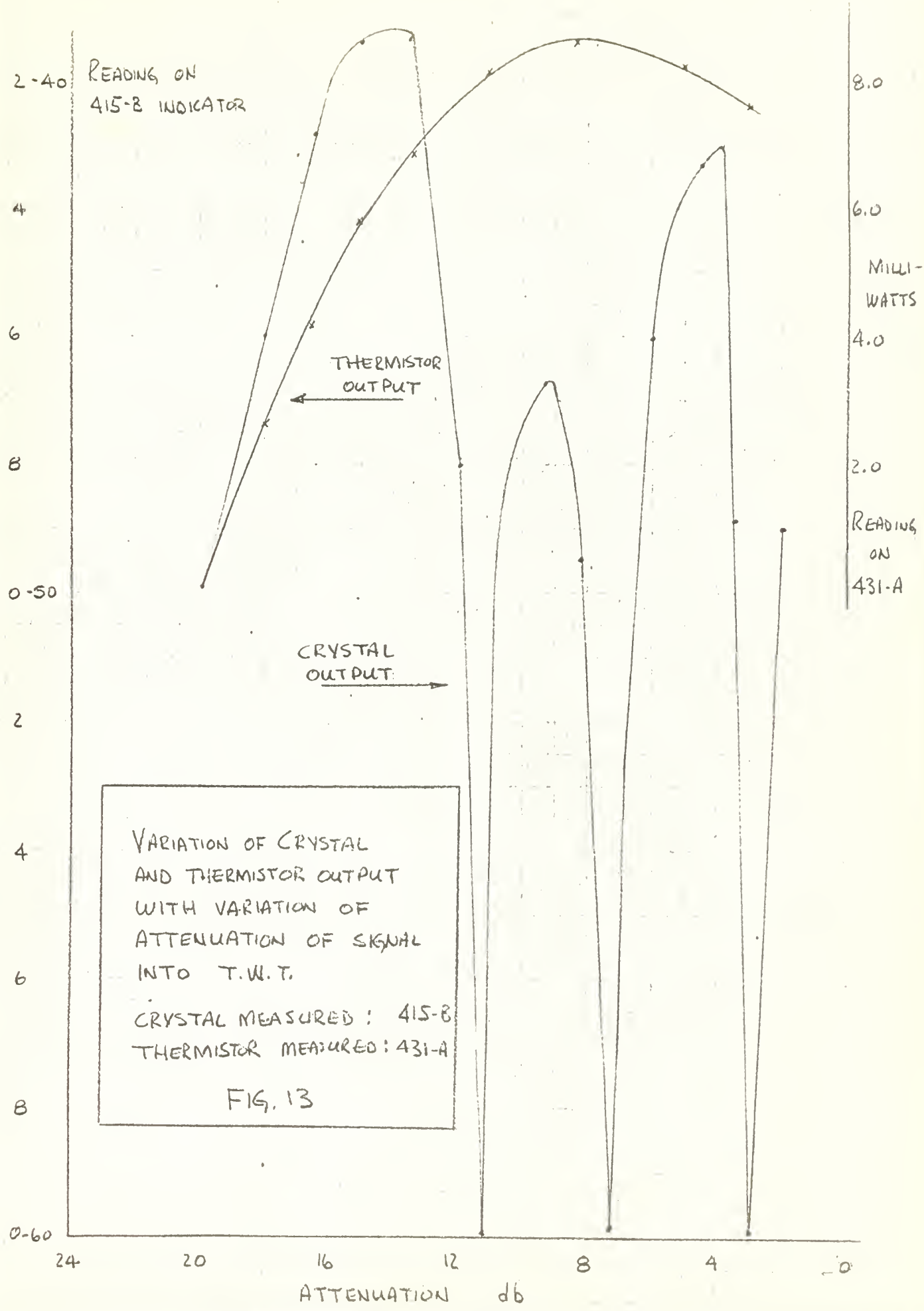

VARIATION OF CRYSTAL AND THERMISTOR OUTPUT WITH VARIATION OF ATTENUATION OF SIGNAL INTO T.W.T.

CRYSTAL MEASURED : 415-B
THERMISTOR MEASURED : 431-A

FIG. 13

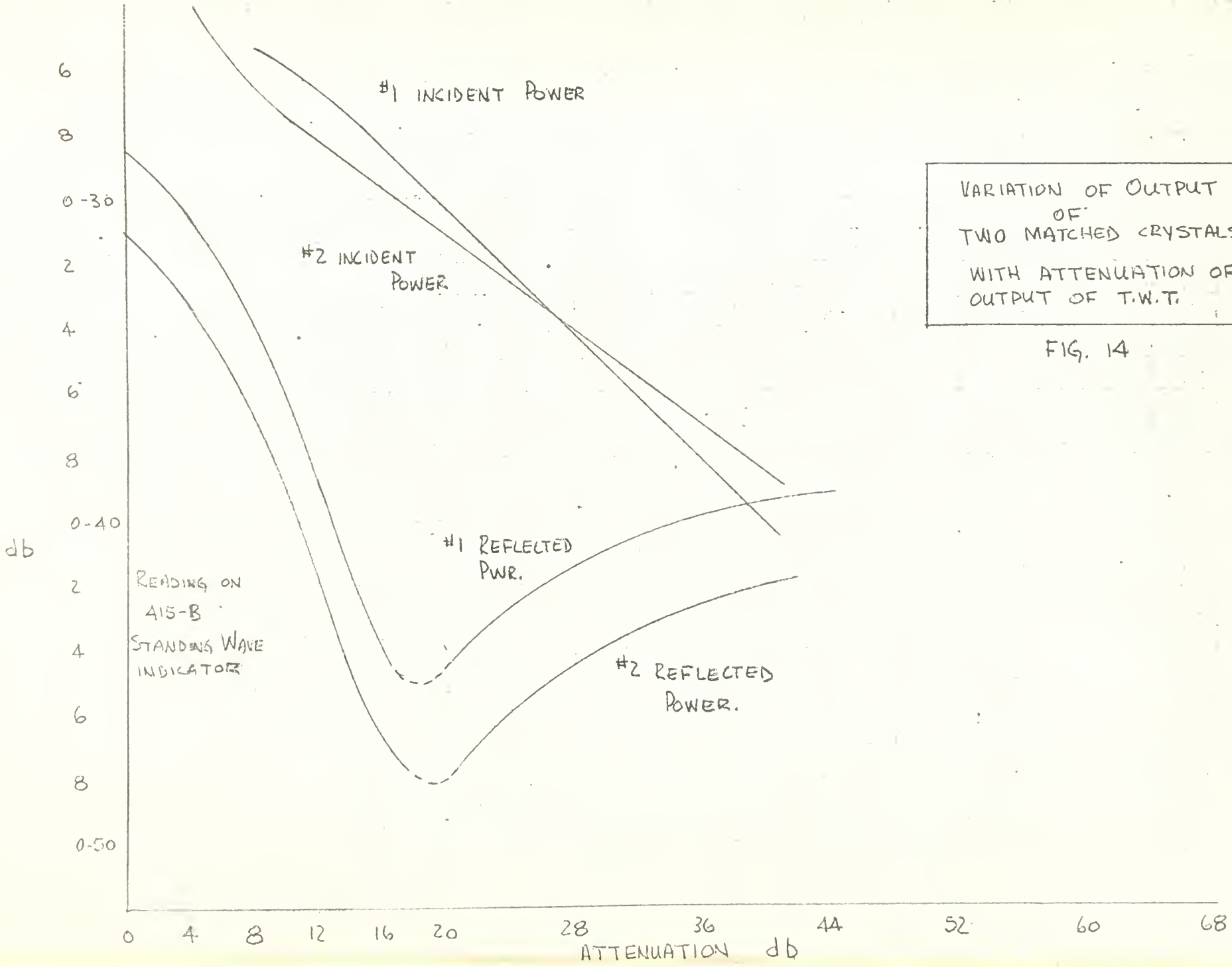

VARIATION OF OUTPUT OF TWO MATCHED CRYSTALS WITH ATTENUATION OF OUTPUT OF T.W.T.

FIG. 14

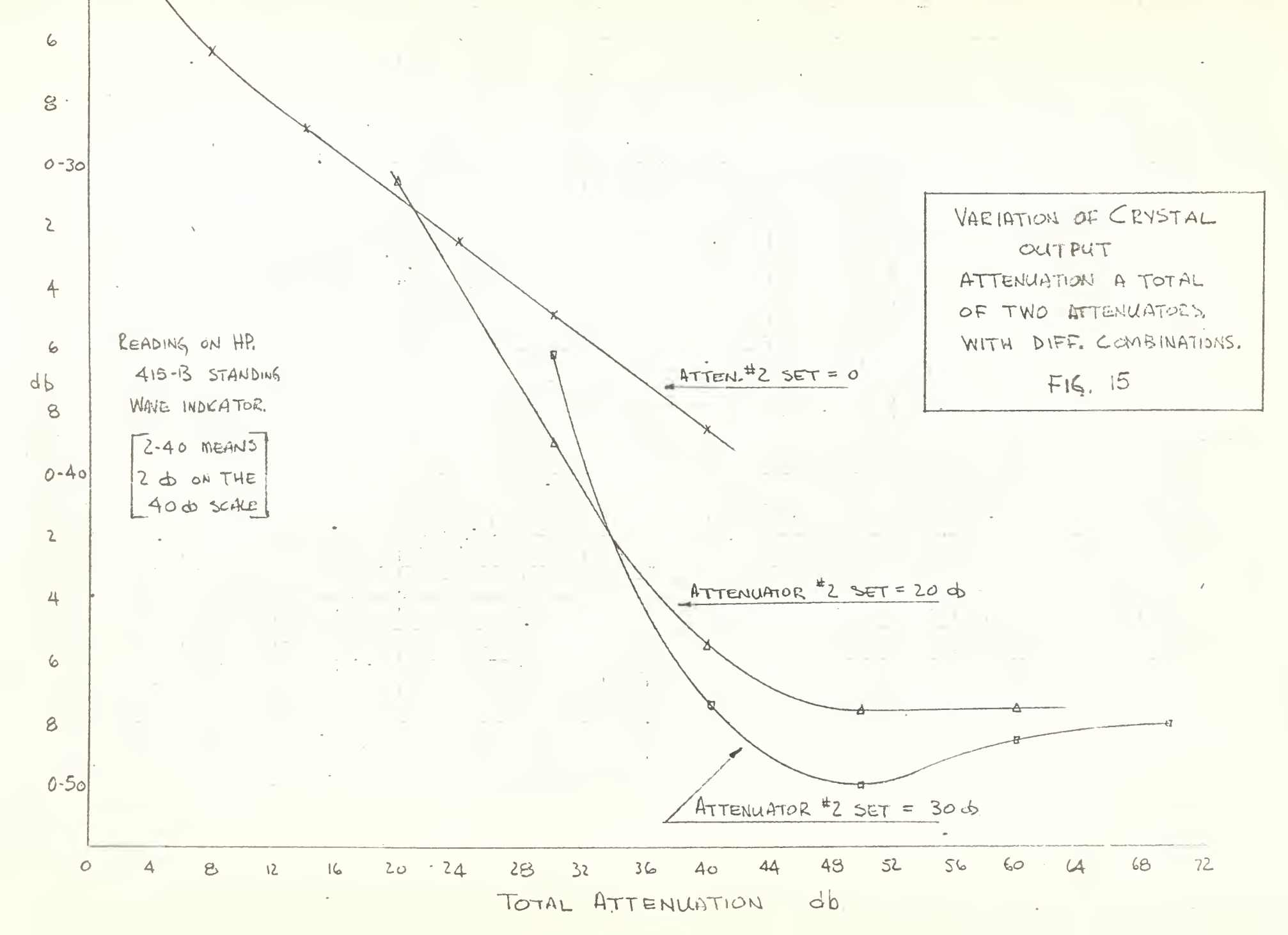
VARIATION OF CRYSTAL OUTPUT ATTENUATION A TOTAL OF TWO ATTENUATORS WITH DIFF. COMBINATIONS.
FIG. 15
READING ON HP. 415-B STANDING WAVE INDICATOR.
2-40 MEANS 2 db ON THE 40 db SCALE
ATTEN. #2 SET = 0
ATTENUATOR #2 SET = 20 db
ATTENUATOR #2 SET = 30 db
6
8
0-30
2
4
6
db
8
0-40
2
4
6
8
0-50
0 4 8 12 16 20 24 28 32 36 40 44 48 52 56 60 64 68 72
TOTAL ATTENUATION db

surements of crystal output.

Now each of the above will be discussed in more detail.

Difficulty a.

The oscilloscope photographs shown in Fig. 12 display the crystal output with 1000 cycle square wave modulation. The crystal, a Hewlett Packard model 421 A Serial 4411 A, was mounted on the reflected channel of a 10 db Hewlett Packard directional coupler. Ten watts were incident on a matched load which was arranged as shown in the schematic of the matching arm shown in Fig.6. View 1 was coincident with a reflected signal down about 30 db from the incident power.

The three oscilloscope views shown were taken with a scale of 0.005 volts per cm., with each square of the grid equal to one cm. View 2 was coincident with a measured value of the reflected signal about 40 db below the incident power; and view 3 was coincident with a reflected signal about 55 db below the incident power. Note that at the time this work was done the later model (431-B) Hewlett Packard Power Meters and their balanced thermistor had not been received and it was not possible to verify these readings of the 415-B Standing Wave Indicator. Since the readings were erratic and could not be confirmed by the model 416 A Ratio Meter, the method could not be applied to the direct measurement of the

scattering coefficients.

Difficulty b.

The graphs shown in Fig. 11 illustrate the sharp dips in measured output of the crystals while varying the attenuation of the signal from the ultra-stable oscillator into the amplifying traveling wave tube.

As shown, these dips were not apparent when the same output power was measured with the thermistor and a HP 431-A power meter. The only possible explanation for this behavior was that the 1000 cycle modulation for the crystal was applied to the f.f. power by a gyraline modulator, model HF 920 Serial 125 which was placed before the attenuator on the input of the tube; and the attenuator effect on the modulation was not linear.

Difficulty c.

As shown in Fig. 12, the output of two crystals, as measured on a Hewlett Packard Standing Wave Indicator model 415-B Serial 007 - 08795, decreased uniformly with decreasing incident power to a certain level, and then increase with a continuing decrease of incident power. The two crystals were mounted on the reflected arm of a 10 db directional coupler and a matched load was used as the termination. Note however that at this point in the work it was still impossible to accurately eliminate the directivity signal in the directional coupler and thus a load could not be accurately matched. The directivity

signal in the directional coupler could have been contributing to this particular difficulty.

Difficulty d.

The non-linearities of two Hewlett Packard attenuators, model X382 A, as measured by crystal Serial 4411-B, are displayed in Fig. 13. Note that non-linearities of this magnitude, (7d), were not detected in similar tests with the Hewlett Packard 431 B power meters.

To perform this test two attenuators were placed between the output of the traveling wave tube and crystal detector. Note that alternate crystals were used to verify this phenomenon. The total attenuation of the two attenuators is plotted as the abscissa and the ordinate indicates the reading on the Hewlett Packard 415 B Standing Wave Indicator, (0.40 means 0 db on the 40 db scale of the meter). For the three curves shown the second attenuator was fixed at 0 db, 20 db, and 30 db respectively. Thus, since the attenuators are essentially linear with r.f. power alone, (no modulation) the same output should have occured with the same total attenuation; particularly in the range at 10 - 30 db on the attenuators. As shown, there was a 5.0 db variation between the three readings at a total attenuation of 30.0 db.

Difficulty e.

The Hewlett Packard Ratio Detector, Model 416 A, was extremely sensitive and often deceiving. On many readings

the needle would indicate a maximum ratio between the two signals being tested and on further checking it would be determined that there was possibly only 20 db variation in the signals but one or the other was too weak for the meter to operate correctly. The issue would be further confused by lack of agreement with the 415-B Standing Wave Indicator.

CHAPTER VI

CONCLUSIONS

It is felt that the results presented in section 4 of this paper verify the work done by Lary /1/ and substantiate the general theory as presented by Kummer /3/, Held /2/, and Silver /4/. The variation of 3.0 db in amplitude and 25.0° degrees in phase between the theoretical and experimental solutions for S_{12}, S_{21}, S_{14}, and S_{23} are attributed to errors in the experimental work introduced by un-wanted coupling in the mode transducers, machining errors, mis-alignment errors, phase errors due to frequency drift, and mismatching of the mode transducers in the TE_{20} mode.

Additional phase errors were undoubtedly introduced by temperature variations along the length of the waveguide system. In this investigation only the readings of the thermometer attached to the arm with rotating joints was used. The readings of an additional thermometer, attached to the supporting frame near port #1, often varied as much as one and one half degrees from the other thermometer but were not taken into account. It is recommended that the waveguide system be reduced in overall length, and that a more extensive temperature monitoring system be installed and employed in correcting the phase data. It is also recommended that mode transducers with isolation of at least 55 db, in contrast to the 35 db

isolation of the existing transducer, be designed and constructed. The slot array junction of two wave guides is suggested as a possible type of transducer. The alignment holes and pins at the two ends of the test section require improvement. In the existing set-up only one alignment pin is available and it is smaller in diameter than some of the alignment holes which are themselves not uniform in size. In addition, alignment holes and pins should be obtained for the junction at port #2 and for each of the matched terminations which are repeatedly removed and replaced in the process of taking measurements.

The procedure for measuring the attenuation employed in this investigation could be improved upon. In every case, one of the two attenuators on either side of magic T "α", as appropriate, was set at zero and the total reading was taken on the other attenuator. The expanded lower scale of the attenuator which had been set at zero should have been used to obtain a more accurate measurement of the difference in amplitude at the two signals at the magic T.

A reliable monitor needs to be constructed for the fan which provides cooling air for the traveling wave tube in order that the system may be left unattended overnight, thus permitting absolute stabilization and reducing the operating hours on the tube. The lack of a reliable monitor during this investigation necessitated excessive

operation of the traveling wave tube for the better part of several days for no useful purpose except warm-up and stabilization of the system. It is felt that the non-directivity of the two couplers used in measuring the reflected signals was accounted for in the numerical corrections presented in section 4. The lack of a TE_{20} matched termination to be used in matching the transducers was also a source of phase and amplitude error. Two isolators were used in the bridge, but since all measurements were taken at the same r.f. power level, they did not contribute to the errors. The maximum frequency deviation of one part in a million of the L F E ultra-stable oscillator, as given in its specifications, meant a maximum deviation of 9,375 cycles at the operating frequency of 9.375 kmc was to be anticipated.

At this frequency, .00885 cm in the waveguide was equivalent to one degree of phase. A frequency variation of 9,375 cycles, could be responsible for about 1.1 degrees error in phase over the approximately 20 feet of waveguide in the bridge. Thus, both a more stable oscillator and a reduction in overall length of the bridge, would help to increase the accuracy of phase measurement.

The close agreement of the three coefficients S_{12}, S_{21} and S_{23}, (less than 0.3^0 degree in phase, and 0.4 db in amplitude) as measured in this investigation, substantiates the accuracy of the bridge as a measuring device and the correctness of the mathematical corrections applied

to the data. When the other difficulties as mentioned above are corrected, the results for particular slots should be in closer agreement with the theory.

APPENDIX A

Port	Incident mode	Atten	∅	Temp corr	corr ∅	Date	Test Section	Short location
Ref	TE_{10}	11.1	346.9	+ 0.2	347.1	10		
		11.1	347.0	0	347.0	12		
		11.2	350.1	- 1.2	348.9	16		
		11.1	347.0	- 0.3	346.7	23		
		11.0	350.0	-2.1	347.9	25		
		11.1			347.0			
Ref	TE_{10}	10.9	326.5	+ 0.2	326.7	23		Z
		10.9	327.0	- 0.1	326.9	23		
		10.9			327			
Ref	TE_{10}	10.4	247.0	+ 1.1	248.1	23		6
		10.42	248.0	- 0.3	247.7	23		
		10.42			248.0			
3	TE_{10}	11.8	279.6	+ 1.2	280.8	12		
		11.7	283.7	- 0.1	283.6	16		
		----	280.3	0	280.3	23		
		11.8	281.1	- 0.2	280.9	25		
		11.8			281.0			
3	TE_{10}	11.6	257.8	+ 2.1	259.9	23		Z
		11.6	257.5	+ 1.9	259.4	23		
		11.6			259.8			
3	TE_{10}	11.21	180.7	+ 1.5	182.2		Guide	6
		11.23	181.4	+ 0.3	181.7			
		11.23	182.0		182.0			

Arithmetic Average Indicated by: [ ]

APPENDIX A

Port	In-cident mode	Atten db	Phase	Date	Test Section	Short Location
3	TE_{20}	9.15	8.1	16	slot	
		9.4	3.8	23		
		9.3	5.0	25		
		9.3	5.0			
4	20	11.82	351.0	16		ϒ
		11.8	342.0	23		
		11.8	345.4	25		
4	20	11.3	190.0	23		Z
		11.36	190.2	23		
		11.36	190.1			
4	TE_{20}	11.0	285.1	23		#5
		11.08	285.1	23		
		11.08	285.1			
4	TE_{20}	-42 +	290.0	22	Guide	
		-45 +	Vague	23		
		-45 +	Vague	25		
		-45.0+	Vague			
4	TE_{20}	1.3	72.0	16	slot	
		1.02	70.0	23		
		1.1	71.0	25		
		1.1	71.0			
5	TE_{20}	21.7	145.8	16	Guide	
		21.7	144.0	23		
		21.6	139.9	23		
		21.7	144.0	25		
		21.7	144.0			

APPENDIX A

Port	Incident Mode	Atten db	Phase	Date	Test Section	Short Location
5	TE_{20}	19.51	153.5	16	Slot	
		19.55	154.0	25		
		19.6	153.4	25		
		19.55	153.5			
6	TE_{20}	-10.8	43.4	22	Guide	
		-12.6	282.9	25		
		-12.6	283.1	25		
		-12.6	283.0			
6	TE_{20}	-0.95	255.9	16	Slot	
		-0.70	256.0	23		
		-0.77	256.5	25		
3	TE_{10}	-35.5	Vague	16	Guide	
		-42.0	Vague	23		
		-42.0	Vague	25		
3	TE_{10}	-23.3	72.3	16	Slot	
		-23.0	70.1	23		
		-22.9	71.4	25		
		-23.0	71.4			
4	TE_{10}	-28.9	26.3	16	Guide	
		-29.0	25.1	22		
		-29.0	24.96	25		
		-29.0	25.0			
4	TE_{10}	-8.91	123.2	16	Slot	
		-8.95	120.98	23		
		-9.10	120.95	25		
		-9.0	121.0			

APPENDIX A

Port	Incident Mode	Atten db	Phase	Date	Test sect'n	Short Location
5	TE_{10}	-11.8	280.8	16	Guide	
		-11.8	278.0	22		
		-11.8	276.8	22		
		-11.8	277.0			
5	TE_{10}	1.65	356.0		Slot	
		1.6	345.5			
		1.6	355.0			
		1.6	355.0			
6	TE_{10}	22.1	149.5	16	Guide	
		21.9	150.1	22		
		21.8	147.8	23		
		21.9	148.0	25		
		21.9	148.0			
6	TE_{10}	21.7	149.3	16	Slot	
		21.5	152.3	25		
		21.6	151.0	25		
		21.6	151.0			
Ref	TE_{20}	10.7	304.0	16		X
		10.7	301.1	23		
		10.6	301.0	25		
		10.65	301.0			
Ref	TE_{20}	10.3	146.1	23		Z
		10.4	145.9	23		
		10.35	146.0			
Ref	TE_{20}	9.97	239.5	23		5
		9.97	239.5			
3	TE_{20}	-21.1	80.2	16	Guide	
		-21.0	79.9	25		
		-21.0	80.0			

APPENDIX B

The following major components were used:

L F E ultra-stable oscillator - Series 814

Specifications:

Stability: One part in 10^6 in frequency

Output: 0.5 watt.

Sperry Traveling Wave Tube - STX - 186

Gain at 9.375 Kmc: 50 db

Saturated Power: 43.2 db m

Uniline Isolators Model X-1225-About 65 db Reverse Isolation.

Hewlett Packard Phase Shifters - Model X-885-A
Serial 1012 (upper arm)
Serial 2128 (lower arm)

Hewlett Packard Attenuators - Model -382-A
Serial 3106 (Ref. Arm)
Serial 3318 (Measuring Arm)

Hewlett Packard Power Meter Models 431 A
Models 431 B

Serial 301 01143
Serial 301 01123
Serial 137 00314
Serial 137 00309

BIBLIOGRAPHY

Lary, R. L., "A Microwave Bridge For The Accurate Measurement of Scattering Matrices Generated By Obstacles In Multimode Waveguides."
Thesis, United States Naval Postgraduate School
May 1962

Held, G., "Scattering by A Slot Radiator In A Multimode Waveguide."
University of California at Berkeley, Institute of Engineering Res., Series #60 No. 114
June 1954

Kammer, W. H. "Measurement Techniques For Multimode Systems and The Properties Of Half Wave Slots In A Two Mode Rectangular Waveguide
University Of California at Berkeley, Institute of Engineering Research. Series #60 No. 135
April 1955

Radiation Laboratory Series, Volume 8

Radiation Laboratory Series, Volume 12

Reich, H. J., "Microwave Principles".
Van Nostrand, D.
Princeton, New Jersey, 1957

thesE773
Measurements of the scattering matrix of
3 2768 001 89198 9
DUDLEY KNOX LIBRARY